

3. Sayago I, Domínguez-Rodríguez F, Oteo-Domínguez JF, Gómez-Bueno M, Segovia J, Alonso-Pulpón L. Dispositivo de asistencia circulatoria Impella CP® como terapia puente a trasplante cardíaco: primera experiencia en España. *Rev Esp Cardiol.* 2015;68:906-908.
4. Dangas GD, Kini AS, Sharma SK, et al. Impact of hemodynamic support with Impella 2.5 versus intra-aortic balloon pump on prognostically important clinical outcomes in patients undergoing high-risk percutaneous coronary intervention (from the PROTECT II randomized trial). *Am J Cardiol.* 2014;113:222-228.

5. Patel NJ, Singh V, Patel SV, et al. Percutaneous coronary interventions and hemodynamic support in the USA: a 5 year experience. *J Interv Cardiol.* 2015;28:563-573.

<http://dx.doi.org/10.1016/j.rec.2016.09.015>  
1885-5857/

© 2016 Sociedad Española de Cardiología. Published by Elsevier España, S.L.U. All rights reserved.

## Performance of a New Software Tool for Automatic Quantification of Left Ventricular Trabeculations



### Rendimiento de un nuevo software para la cuantificación automática de trabeculaciones en el ventrículo izquierdo

#### To the Editor,

We aimed to evaluate the performance of the first published software tool<sup>1</sup> for the automatic quantification of left ventricular noncompaction (LVNC) based on automatic delineation of the epicardial and endocardial borders of the left ventricular (LV) and trabecular recesses.

Twenty-one LVNC patients meeting Petersen's criteria<sup>2</sup> were compared with 14 control individuals (relatives not meeting LVNC criteria who were free from family mutations). Eleven (52.3%) of the affected patients had systolic dysfunction (8 of those with LV dilatation), 1 had dilatation without systolic impairment, and 1 had LV hypertrophy (20-mm maximum wall thickness). Ten individuals had isolated hypertrabeculation meeting LVNC criteria (Table).

Cardiac magnetic resonance cine images (repetition interval of 2.8 ms, echo time of 1.4 ms, flip of 60°, matrix of 190 x 200, echo train length of 23, cutting thickness of 8 mm, with 30 phases) were reviewed by 2 experienced investigators independently. Fourteen (5.8%) of 242 slices were of insufficient quality. Short axis slices, from the apex to the mitral annulus in end-diastole were analyzed with dedicated software. A standard protocol was used for measurements of LV volumes and wall thickness.

Delineation of the endocardial border, endocardial compacted layer, and pericardial border was performed automatically.<sup>1</sup> The trabecular zones are detected inside and around the LV cavity. The software produces measurements of area, volume, and estimates of mass of compacted and noncompacted LV myocardium per slice, and total LV. All measurements are presented as absolute values and are indexed by body surface area. The proportion of trabeculated mass from total LV mass was also calculated. Delineation of the borders was subjectively scored by 2 skilled cardiologists.

The LVNC patients and control groups showed significant differences in the trabeculated layer mass in most apical and mid slices (slices 2-6) both for absolute and indexed values (Figure). Although the percentage of trabeculation was higher in all slices, it was significant only for apical slices 2 and 3 and basal slice 8. There was no difference in the compacted layer between groups.

When slices were grouped into apical, mid and basal and all 3 segments showed significantly higher values for absolute trabeculated layer, indexed trabeculated layer and percentage of trabeculation in the LVNC group. As with individual slices, there were no differences in the mass of the compacted layer by segments between groups.

The trabeculated layer and percentage of trabeculation was significantly higher in LVNC patients than in the control group (86.6 ± 27.4 g vs 56.1 ± 24.4 g;  $P = .002$  and 32.3 ± 4.6% vs 25.0 ± 7.7%;  $P = .001$ , respectively).

On multivariate analysis, the indexed trabeculated layer was the variable independently associated with the diagnosis of LVNC (hazard ratio, 1.11; 95% confidence interval, 1.03-1.19;  $P = .009$ ).

Receiver operating characteristics curve analysis of the 2 variables that differentiated LVNC patients and controls was performed to identify cutoff values. These were 0.82 (95% confidence interval, 0.67-0.96;  $P = .002$ ) for the indexed trabeculated layer and 0.78 (95% confidence interval, 0.61-0.95;  $P = .006$ ) for the percentage of trabeculation. A cutoff value of 40.0 g/m<sup>2</sup> of the indexed trabeculated layer had a sensitivity of 81.0% and a specificity of 78.6%. Similarly, a cutoff value of 27.4% of the percentage of trabeculation had a sensitivity of 90.5% and a specificity of 71.4%.

All (88.6%) but 4 individuals from the total of 35 individuals were appropriately classified. Seventeen (81.0%) of the 21 LVNC patients had values above the 2 cutoffs, and 2 (9.5%) reached only 1 of them.

The performance of the automatic software was evaluated first by the engineers and then by cardiac magnetic resonance expert cardiologists, with very good visual agreement in 96% of the slices. Trabeculation was particularly prominent in apical slices with a

**Table**  
Baseline Characteristics and Summary of Results

	Controls	LVNC patients	P
N	14 (40.0%)	21 (60.0%)	
Male/female	7/7	12/9	.7
Age	32.4 ± 13.6	41.5 ± 12.2	.05
BSA, m <sup>2</sup>	1.69 ± 0.18	1.73 ± 0.19	.05
iLVED, mL/m <sup>2</sup>	81.6 ± 16.9	97.3 ± 15.1	.01
iLVES, mL/m <sup>2</sup>	37.2 ± 12.1	53.0 ± 14.7	.005
LVEF, %	55.0 ± 8.2	46.1 ± 9.9	.02
Trabeculated layer, g	56.1 ± 24.4	86.6 ± 27.4	.002
iTrabeculated layer, g/m <sup>2</sup>	32.7 ± 12.1	50.0 ± 15.7	.001
Compacted layer, g	169.6 ± 48.7	183.3 ± 60.8	.5
iCompacted layer, g/m <sup>2</sup>	100.2 ± 26.3	106.0 ± 36.2	.6
Trabeculation, %	25.0 ± 7.7	32.3 ± 4.6	.001
iTrabeculated layer, g/m <sup>2</sup>			
Apical	4.1 ± 2.2	7.2 ± 3.1	<.00001
Mid	6.1 ± 2.0	8.6 ± 2.5	<.00001
Basal	4.6 ± 3.0	6.4 ± 3.4	.03
iCompacted layer, g/m <sup>2</sup>			
Apical	10.2 ± 3.4	10.9 ± 4.1	.3
Mid	15.6 ± 3.2	17.3 ± 5.2	.1
Basal	18.2 ± 2.6	19.2 ± 5.5	.3
Trabeculation, %			
Apical	28.7 ± 11.6	39.2 ± 10.0	<.00001
Mid	28.2 ± 8.9	33.4 ± 6.4	.008
Basal	19.0 ± 11.5	24.4 ± 9.7	.04

BSA, body surface area; i, BSA indexed; iLVED: indexed left ventricular end-diastolic volume; iLVES, indexed left ventricular end systolic volume; LVEF, left ventricular ejection fraction; LVNC, left ventricular noncompaction.

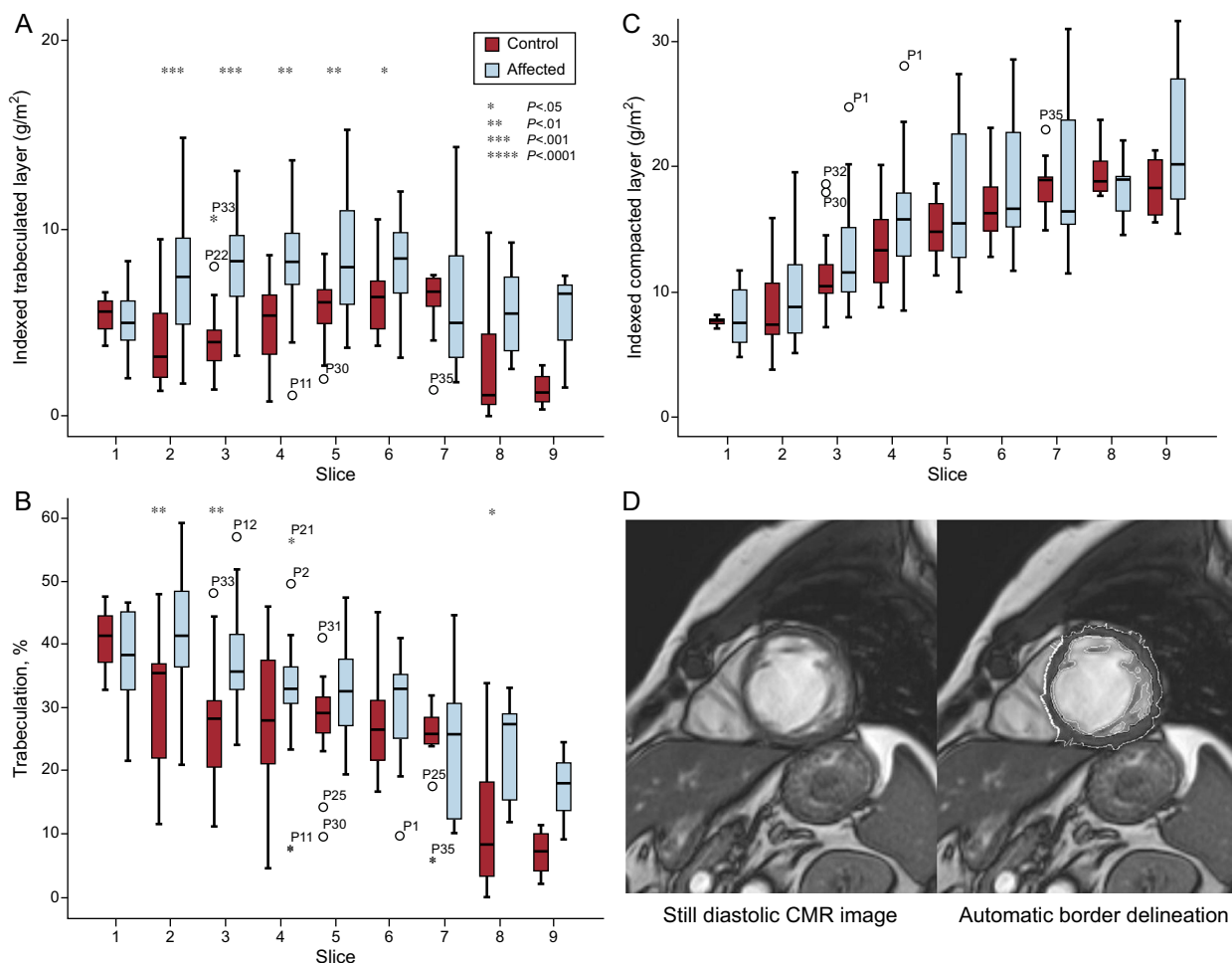


**Figure.** A-B: Differences in indexed trabeculated layer and compacted layer per slice in LVNC patients and controls. C-D: Delineation of the endocardial border, endocardial compacted layer and pericardial border was performed automatically by the software. CMR, cardiac magnetic resonance; LVNC, left ventricular noncompaction.

75.6% increase in indexed trabeculated layer in LVNC patients vs the control group, followed by mid and basal segments (41.0% and 39.1%, respectively). The indexed trabeculated layer seems to perform better than the percentage of trabeculation.

Although most definitions of LVNC include a thin, hypokinetic compacted layer in the criteria, we failed to identify any differences, either by slice or globally, in the measurement of compacted myocardium between LVNC patients and controls.

Our automatic software established a higher cutoff of trabeculation (27%) compared with that proposed by Jacquier (20%) using hand delineation of borders.<sup>3</sup> With a similar method, Choi et al.<sup>4</sup> published a cutoff of 35% in volume trabeculation, when comparing between different groups of cardiomyopathies. Neither of these authors used a trabecula-dedicated software of quantification.

In contrast to the fractal analysis recently published by Captur et al.,<sup>5</sup> based on tortuosity measured by pixilation of the line of the endocardial border, our software provides easy to understand clinical measurements of volumes and masses of the compacted and noncompact LV myocardium. This computationally-assisted method could save valuable diagnostic time compared with traditional processing, thus minimizing the possibility of human error.

In conclusion, we demonstrate the good performance of a new software tool for quantification of hypert trabeculation based on the automatic delineation of borders from cardiac magnetic resonance diastolic images. Cutoffs of normality were established according

to trabeculated mass and percentage of trabeculation. Further confirmatory studies are needed.

*Acknowledgements*

The investigators are part of a cardiovascular research network of the Carlos III Health Institute (RIC; RD12/0042/0049). This work was supported by the Spanish MINECO, as well as European Commission FEDER funds, under grant TIN2015-66972-C5-3-R.

Gregorio Bernabé García,<sup>a,\*</sup> Josefa González-Carrillo,<sup>b</sup> Javier Cuenca Muñoz,<sup>a</sup> Daniel Rodríguez Sánchez,<sup>c</sup> Daniel Saura Espín,<sup>b</sup> and Juan Ramón Gimeno Blanes<sup>b</sup>

<sup>a</sup>Departamento de Ingeniería y Tecnología de Computadores, Facultad de Informática, Universidad de Murcia, Murcia, Spain  
<sup>b</sup>Unidad de Cardiopatías Familiares, Servicio de Cardiología, Hospital Universitario Virgen de la Arrixaca, El Palmar, Murcia, Spain  
<sup>c</sup>Servicio de Radiología, Hospital Universitario Virgen de la Arrixaca, El Palmar, Murcia, Spain

\* Corresponding author:  
 E-mail address: [gbernabe@dittec.um.es](mailto:gbernabe@dittec.um.es) (G. Bernabé García).

Available online 27 August 2016

REFERENCES

- Bernabé G, Cuenca J, de Teruel PEL, Giménez D, González-Carrillo J. A Software Tool for the Automatic Quantification of the LV Myocardium Hyper-trabeculation Degree. *Procedia Comput Sci.* 2015;51:610-619.
- Petersen SE, Selvanayagam JB, Wiesmann F, et al. LVNC: insights from cardiovascular magnetic resonance imaging. *J Am Coll Cardiol.* 2005;46:101-105.
- Jacquier A, Thuny F, Jop B, et al. Measurement of trabeculated LV mass using CMR imaging in the diagnosis of LVNC. *Eur Heart J.* 2010;31:1098-1104.
- Choi Y, Kim SM, Lee SC, Chang SA, Jang SY, Choe YH. Quantification of LV trabeculae using CMR for the diagnosis of LVNC: evaluation of trabecular volume and refined semi-quantitative criteria. *J Cardiovasc Magn Reson.* 2016;18:24.

- Captur G, Lopes LR, Patel V, et al. Abnormal Cardiac Formation in Hypertrophic Cardiomyopathy-Fractal Analysis of Trabeculae and Preclinical Gene Expression. *Circ Cardiovasc Genet.* 2014;7:241-248.

<http://dx.doi.org/10.1016/j.rec.2016.07.006>  
1885-5857/

© 2016 Sociedad Española de Cardiología. Published by Elsevier España, S.L.U. All rights reserved.

**Coronary-myocardial-valvular Percutaneous Intervention**



**Intervención coronaria-miocárdica-valvular percutánea**

**To the Editor,**

Substantial progress in transcatheter cardiac interventions has allowed the treatment of a large number of patients with poor surgical prognosis. Comorbidities, frailty, and concurrent cardiac diseases in elderly patients often limit the option of surgery. Some patients with these factors are considered inoperable while others are deemed at high surgical risk. The indication for intervention in

this latter group of patients is subject to debate, as the decision depends on assessment of a given multidisciplinary team and agreement by a specific surgical team. We describe the case of an inoperable female patient with several cardiac diseases who was successfully treated by percutaneous intervention, with subsequent clinical improvement.

A 70-year-old woman, diagnosed with long-standing obstructive hypertrophic cardiomyopathy and in New York Heart Association functional class II was admitted to hospital for the first time in March 2013 with heart failure (HF) associated with atrial fibrillation. Electric cardioversion was effective. Subsequently, in the same year, she was hospitalized once again due to HF with preserved sinus rhythm. The electrocardiogram showed severe,

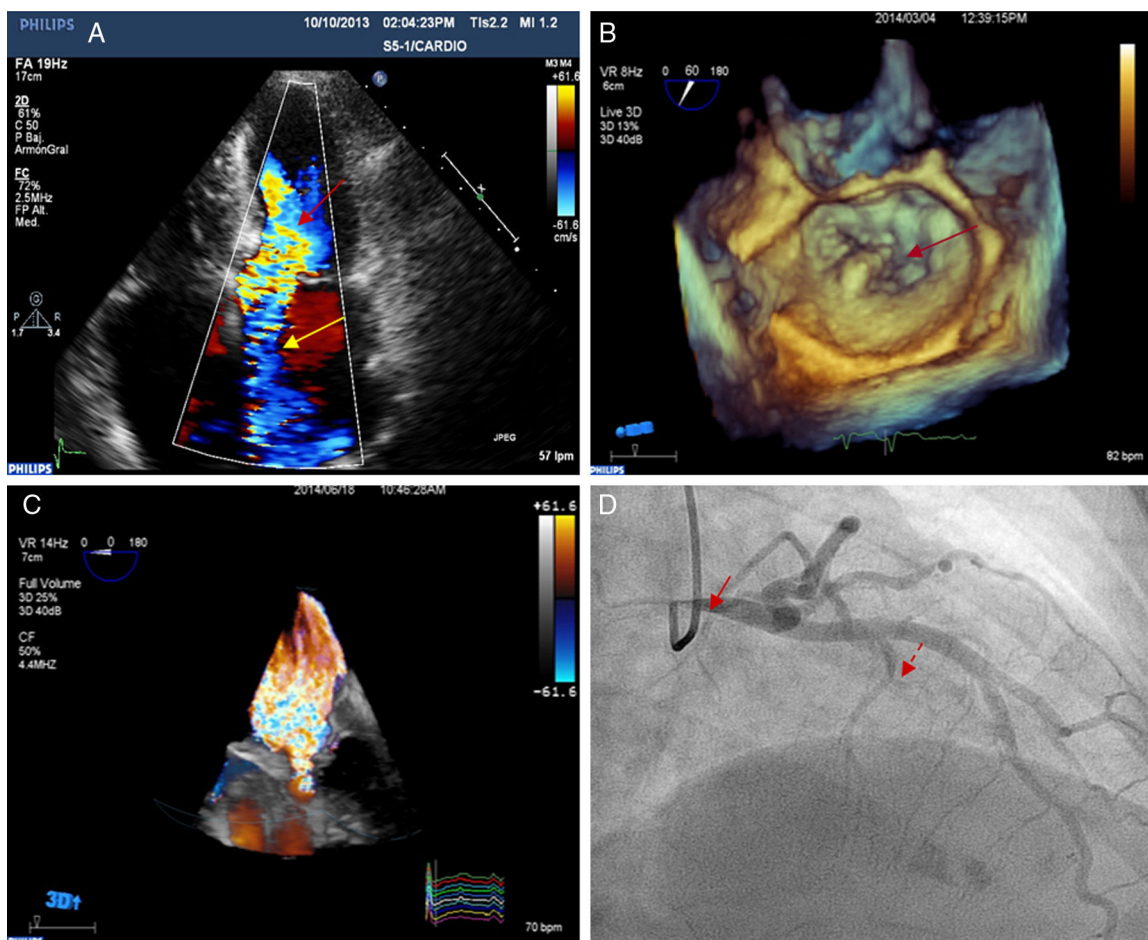


**Figure 1.** A: transthoracic echocardiogram showing dynamic obstruction of the left ventricle (red arrow) and mitral valve regurgitation in the anteroseptal direction due to organic valve disease (yellow arrow). B: 3-dimensional transesophageal echocardiogram with 3-dimensional zoom showing posterior mitral leaflet prolapse (arrow). C: 3-dimensional, full volume, color Doppler transesophageal echocardiogram showing severe mitral valve regurgitation. D: coronary angiography, 30° right anterior oblique view showing severe stenosis of the left main coronary artery (solid arrow) and septal branch treated with alcohol ablation (dashed arrow).